Journal of Solution Chemistry (2018) 47:2082–2093
https://doi.org/10.1007/s10953-018-0826-9

Synthesis, Micellar and Surface Properties of Cationic Trisiloxane Surfactants with Different Siloxane Hydrophobic Groups

Jinglin Tan[1] · Miaomiao Lin[1] · Zhigang Ye[1]

Received: 27 April 2018 / Accepted: 2 October 2018 / Published online: 16 November 2018

Abstract
Three cationic trisiloxane surfactants, 1-methyl-1-[bis(trimethylsiloxy)methyl]silyl-propylpyrrolidinium chloride (Si_3pyCl), 1-methyl-1-[bis(triethylsiloxy)methyl]silyl-propylpyrrolidinium chloride (Et-Si_3pyCl), and 1-methyl-1-[bis(vinyldimethylsiloxy)methyl]silyl-propylpyrrolidinium chloride (Vi-Si_3pyCl) were synthesized. The aggregation behavior of the trisiloxane surfactants with different siloxane hydrophobic groups in aqueous solution was investigated by surface tension and electrical conductivity measurements. The structures of hydrophobic groups of the trisiloxane surfactants can obviously influence their surface activities and thermodynamics. All the three cationic trisiloxane surfactants have excellent surface activity. Owing to the steric hindrance of hydrophobic groups, the *CMC* values increase following the order Et-Si_3PyCl < Vi-Si_3PyCl < Si_3PyCl. The ΔG^{o}_{m} values increase in the order Et-Si_3PyCl > Vi-Si_3PyCl > Si_3PyCl, attributed to the decrease in the hydrophobic effect. The micellization processes of these surfactants are entropy-driven.

Keywords Trisiloxane surfactants · Steric hindrance · Surface activity

1 Introduction

Silicone surfactants are novel efficient amphiphilic materials that consist of siloxane as hydrophobic group attached to one or more hydrophilic groups [1–3]. Because of their unique chemical and physical properties, such as superspreading behavior and abilities to decrease the surface tension of water to approximately 20 $mN{\cdot}m^{-1}$, silicone surfactants have been widely investigated and used during the past decades. Especially trisiloxane surfactants are under the spotlight [4–7].

Electronic supplementary material The online version of this article (https://doi.org/10.1007/s10953-018-0826-9) contains supplementary material, which is available to authorized users.

✉ Jinglin Tan
tmeizi@hotmail.com

[1] Jiangxi Province Engineering Research Center of Ecological Chemical Industry, School of Chemical and Environmental Engineering, Jiujiang University, Jiujiang 332005, Jiangxi, China

In recent years, the aggregation behavior of silicone surfactants in aqueous solution has been increasingly investigated. Du et al. [8–11] reported that trisiloxane cationic silicone surfactants can form vesicular aggregates with diameters from 20 to 200 nm. In addition, butynediol-ethoxylate based silicone surfactants show excellent surface activity, spreading and wetting ability in comparison with acetylenic diol surfactants. It is worth noting that a growing number of silicone surfactants with different hydrophilic groups, such as glucosamide and sugar, have been reported [12, 13].

Zhao et al. [14] reported branched tetrasiloxane based Gemini imidazolium surfactants can reduce the surface tension of water to 20 to 24 $mN{\cdot}m^{-1}$. The micellization process is entropy driven and it can form aggregates with sizes of approximately 100 nm. Feng [15–19] et al. reported a series of cationic silicone surfactants with different hydrophobic groups (permethylated siloxanes including branched siloxanes), hydrophilic groups and counterions. It was concluded that the cationic silicone surfactants have excellent surface activities. The molecular structures of cationic silicone surfactants remarkably affect the aggregation behavior of cationic silicone surfactants in aqueous solution. Notably, the values of degree of counterion binding for (2-hydroxyethyl)-*N*,*N*-dimethyl-3-[tri(trimethylsiloxy)]silylpropyl-ammonium chloride and 1-methyl-1-[tri-(trimethylsiloxy)]silylpropylpyrrolidinium chloride increase with increasing temperature, which is caused by the attractive interaction between the nitrogen atom of one surfactant molecule with the oxygen atom of another surfactant molecule. In addition, the effect of inorganic and organic salts on the aggregation behavior of cationic silicone surfactants have been investigated, indicating that spherical aggregates with diameters from 150 to 600 nm are formed, and the aggregate size decreases upon addition of inorganic and organic salts.

To the best of our knowledge, the hydrophobic groups of the studied silicone surfactants are almost all permethylated siloxane groups. Few systematic and detailed reports about the effect of non-permethylated siloxane groups on the aggregation behavior of cationic silicone surfactants in aqueous solution have been reported.

In the present work, three cationic silicone surfactants with non-permethylated siloxane hydrophobic groups, 1-methyl-1-[bis(trimethylsiloxy)methyl]-silylpropylpyrrolidinium chloride (Si_3pyCl), 1-methyl-1-[bis(triethylsiloxy)methyl]-silylpropylpyrrolidinium chloride (Et-Si_3pyCl), and 1-methyl-1-[bis(vinyldimethyl-siloxy)methyl]silylpropylpyrrolidinium chloride (Vi-Si_3pyCl), were synthesized and utilized to investigate the effect of non-permethylated siloxane hydrophobic groups on the aggregation behavior of silicone surfactants.

2 Experimental Section

2.1 Materials

γ-Chloropropylmethyldichlorosilane (97%) was purchased from Jiangxi Chenguang New Materials Co., Ltd. Chlorotrimethylsilane (98%), chlorotriethylsilane (97%), chlorodimethylvinylsilane (97%), and *N*-methylpyrrolidine (98%) were purchased from Tokyo Chemical Industry Co., Ltd. Methanol (99.5%), isopropanol (99.7%), and *n*-hexane (97%) were obtained from Sinopharm Chemical Reagent Beijing Co., Ltd. All reagents were used as received. Triply distilled water was used to prepare all the solutions. The structures of the cationic silicone surfactants used in this work are shown in Fig. 1.

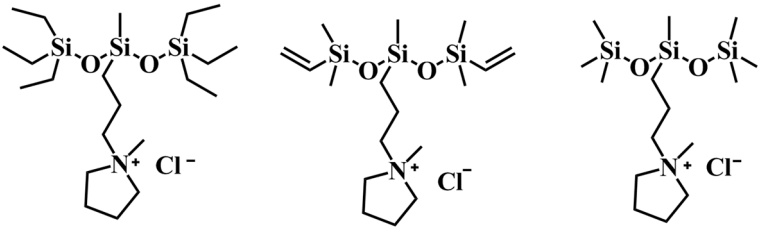

Fig. 1 Chemical structures of the three cationic silicone surfactants

2.2 Preparation of γ-Chloropropyldi(trimethylsiloxy)methylsilane

A mixture of chlorotrimethylsilane (0.2 mol, 21.73 g) and γ-chloropropylmethyldichlorosil ane (0.05 mol, 9.58 g) was mixed into a flask and isopropanol (0.3 mol, 18.0 g) was added. Then water (0.3 mol, 5.4 g) was slowly added to the resulting alkoxylated reaction product. After 5 h, the organic layer was separated from the hydrolysate, washed until it was neutral, and distilled in vacuum to provide γ-chloropropyldi(trimethylsiloxy)methylsilane. The product was confirmed by ^{1}H NMR and FT-IR. ^{1}H NMR ($CDCl_3$): 0.05–0.12 ppm (Si$\boldsymbol{CH_3}$, 21 H), 0.57–0.61 ppm (C$\boldsymbol{H_2}$$CH_2CH_2Cl$, 2 H), 1.77–1.85 ppm ($CH_2C\boldsymbol{H_2}CH_2Cl$, 2 H), 3.50–3.54 ppm ($H_2CH_2C\boldsymbol{H_2}Cl$, 2 H); IR (KBr, cm^{-1}): 2957, 2897, 1258, 1060, 846, 760, 686, 590.

2.3 Preparation of γ-Chloropropyldi(triethylsiloxy)methylsilane

A mixture of chlorotriethylsilane (0.2 mol, 30.14) of and γ-chloropropylmethyldichloro silane (0.05 mol, 9.58 g) was mixed into a flask and isopropanol (0.3 mol, 18.0 g) was added. Then, water (0.3 mol, 5.4 g) was slowly added to the resulting alkoxylated reaction product. After 6 h the organic layer was separated from the hydrolysate, washed until it was neutral, and distilled under vacuum to provide γ-chloropropyldi(triethylsiloxy) methylsilane. The product was confirmed by ^{1}H NMR and FT-IR. ^{1}H NMR ($CDCl_3$): δ (ppm) = 0.13 (Si$\boldsymbol{CH_3}$, 3 H), 0.70–0.75 (C$\boldsymbol{H_2}$$CH_2CH_2Cl$, 2 H), 1.19–1.24 ($CH_2C\boldsymbol{H_3}$, 18 H), 1.79–1.90 ($CH_2C\boldsymbol{H_2}CH_2Cl$, 2 H), 3.50–3.54 ($H_2CH_2C\boldsymbol{H_2}Cl$, 2 H), 3.73–3.80 (C$\boldsymbol{H_2}CH_3$, 12 H); IR (KBr, cm^{-1}): 2973, 2925, 2882, 1261, 1109, 1079, 949, 817, 797, 766.

2.4 Preparation of γ-Chloropropyldi(dimethylvinylsiloxy)methylsilane

A mixture of of chlorodimethylvinylsilane (0.2 mol, 24.13 g) and γ-chloropropylmethyldichloro-silane (0.05 mol, 9.58 g) was mixed in a flask and isopropanol (0.3 mol, 18.0 g) was added. Then, water (0.3 mol, 5.4 g) was slowly added to the resulting alkoxylated reaction product. After 4 h, the organic layer was separated from the hydrolysate, washed until it was neutral, and distilled under vacuum to provide γ-ch loropropyldi(dimethylvinylsiloxy)methylsilane. The product was confirmed by ^{1}H NMR and FT-IR. ^{1}H NMR ($CDCl_3$): 0.05–0.19 ppm (Si$\boldsymbol{CH_3}$, 15 H), 0.55–0.57 ppm (C$\boldsymbol{H_2}$CH-$_2CH_2Cl$, 2 H), 1.74–1.84 ppm ($CH_2C\boldsymbol{H_2}CH_2Cl$, 2 H), 3.47–3.52 ppm ($H_2CH_2C\boldsymbol{H_2}Cl$, 2 H),

5.68–5.77 ppm and 6.07–6.18 ppm ($C\boldsymbol{H_2}$=CH, 4 H), 5.90–5.98 ppm (CH_2=$\boldsymbol{CH}$, 2 H); IR (KBr, cm^{-1}): 3076, 2964, 2900, 1260, 1061, 828, 787, 688, 591.

2.5 Synthesis of Si_3PyCl

γ-Chloropropyldi(trimethylsiloxy)methylsilane (0.01 mol, 2.99 g) together with a 2.5-fold molar excess of *N*-methylpyrrolidine (0.025 mol, 2.02 g) in 6 mL isopropanol were mixed in a flask and refluxed at 85 °C under stirring for 40 h. The excess *N*-methylpyrrolidine and solvent were removed by distilling under vacuum. The crude solid was purified by reprecipitation from methanol and hexane. The pure Si_3pyCl (solid) was confirmed by ^{1}H NMR, ^{13}C NMR, ^{29}Si NMR, FT-IR, and ESI–MS. ^{1}H NMR ($CDCl_3$): δ (ppm) = 0.03–0.12 (Si$\boldsymbol{CH_3}$, 21H), 0.46–0.52 (Si$\boldsymbol{CH_2}CH_2$, 2H), 1.67–1.78 ($SiCH_2\boldsymbol{CH_2}$, 2H), 2.24–2.44 ($\boldsymbol{CH_2}N\boldsymbol{CH_2}$, 4H), 3.30 (N$\boldsymbol{CH_3}$, 3H), 3.50–3.56 ($SiCH_2CH_2\boldsymbol{CH}$, 2H), 3.67–3.75 ($NCH_2\boldsymbol{CH_2}$, 2H), 3.87–4.02 ($NCH_2\boldsymbol{CH_2}$, 2H). ^{29}Si NMR ($CH_3OD$): δ (ppm) = 8.18 ($\boldsymbol{Si}(CH_3)_3$), –22.89 ($\boldsymbol{Si}CH_3$). ^{13}C NMR ($CH_3OD$): δ (ppm) = 67.30 ($SiCH_2CH_2\boldsymbol{C}H$), 64.75 ($\boldsymbol{C}H_2N\boldsymbol{C}H_2$), 48.21 (N$\boldsymbol{C}$H), 21.91 (Si$\boldsymbol{C}H_2CH_2$), 18.34 ($NCH_2\boldsymbol{C}H_2$), 14.36 ($SiCH_2\boldsymbol{C}H_2$), 1.28 (Si($\boldsymbol{C}H_3)_3$), 0.88 (Si$\boldsymbol{C}H_3$). IR (KBr, cm^{-1}): 2957, 2896, 1255, 1042, 840, 754. ESI–MS: calculated, 348.22 g·mol^{-1}; found, 348.22.

2.6 Synthesis of Et-Si_3PyCl

Et-Si_3PyCl was prepared by a similar procedure to that of Si_3PyCl. Briefly, γ-chloropropyl tri(triethylsiloxy)silane (0.01 mol, 3.83 g) together with a 2.5-fold molar excess of *N*-methylpyrrolidine (0.025 mol, 2.02 g) in 8 mL isopropanol was mixed in a flask and refluxed at 85 °C under stirring for 48 h. The excess *N*-methylpyrrolidine and solvent were removed by distilling under vacuum. The crude solid was purified by reprecipitation from methanol and hexane. The pure Et-Si_3PyCl (paste) was dried in vacuo at 40° for 8 h and confirmed by ^{1}H NMR, ^{13}C NMR, ^{29}Si NMR, FT-IR, and ESI–MS. ^{1}H NMR (CD_3OD): δ (ppm) = 0.03 (Si$\boldsymbol{CH_3}$, 3 H), 0.46–0.57 (Si$\boldsymbol{CH_2}CH_2$, 2H), 1.05–1.14 ($CH_2\boldsymbol{CH_3}$, 18 H), 1.68–1.76 ($SiCH_2\boldsymbol{CH_2}$, 2H), 2.24–2.41 ($\boldsymbol{CH_2}N\boldsymbol{CH_2}$, 4), 3.58 (N$\boldsymbol{CH_3}$), 3.07–3.08 ($SiCH_2CH_2\boldsymbol{CH}$, 2H), 3.24–3.26 (C$\boldsymbol{H}_2CH_3$, 12 H), 3.59–3.68 ($NCH_2\boldsymbol{CH_2}$), 3.94–4.06 ($NCH_2\boldsymbol{CH_2}$). ^{13}C NMR ($CH_3OD$): δ (ppm) = 68.30 ($SiCH_2CH_2\boldsymbol{C}H$), 65.45 ($\boldsymbol{C}H_2N\boldsymbol{C}H_2$), 49.11(N$\boldsymbol{C}$H), 22.89 (Si$\boldsymbol{C}H_2CH_2$), 19.15 ($NCH_2\boldsymbol{C}H_2$), 16.21 ($SiCH_2\boldsymbol{C}H_2$), 10.28 (Si($\boldsymbol{C}HCH_3$), 2.31 (Si(CH$\boldsymbol{C}H_3$), 0.78 (Si$\boldsymbol{C}H_3$). ^{29}Si NMR ($CH_3OD$): δ (ppm) = 6.05 ($\boldsymbol{Si}CH_2CH_3$), –22.75 ($\boldsymbol{Si}CH_3$). IR (KBr, cm^{-1}): 2972, 2923, 2866, 1259, 1061, 869, 794,764. ESI–MS: calculated, 432.31 g·mol^{-1}; found, 432.32.

2.7 Synthesis of Vi-Si_3PyCl

Vi-Si_3PyCl was prepared by an analogous procedure to that of Si_3PyCl. γ-Chloropro pyldi(dimethylvinylmethylsiloxy)methylsilane (0.01 mol, 3.23 g) together with a 2.5-fold molar excess of *N*-methylpyrrolidine (0.025 mol, 2.02 g) in 8 mL isopropanol was mixed in a flask and refluxed at 85 °C under stirring for 48 h. Then, the excess *N*-methylpyrrolidine and solvent were removed by distilling under vacuum. The crude solid was purified by reprecipitation from methanol and hexane. The pure Vi-Si_3PyCl (paste) was confirmed by ^{1}H NMR, ^{13}C NMR, ^{29}Si NMR, FT-IR, and ESI–MS. ^{1}H NMR ($CDCl_3$): δ (ppm) = 0.03–0.20 (Si$\boldsymbol{CH_3}$, 15H), 0.49–0.55 (Si$\boldsymbol{CH_2}CH_2$, 2H), 1.68–1.76 ($SiCH_2\boldsymbol{CH_2}$,

2H), 2.24–2.32 ($\boldsymbol{CH_2}N\boldsymbol{CH_2}$, 4H), 3.30 ($N\boldsymbol{CH_3}$, 3H), 3.46–3.564 ($SiCH_2CH_2\boldsymbol{CH}$, 2H), 3.71–3.78 ($NCH_2\boldsymbol{CH_2}$), 3.89–3.93 ($NCH_2\boldsymbol{CH_2}$), 5.67–5.78, and 6.05–6.16 ($\mathbf{CH_2}$=CH, 4H), 5.91–5.98 (CH_2=C**H**, 2H). ^{29}Si NMR (CH_3OD): δ (ppm) = − 3.08 ($\boldsymbol{Si}CH_2$=CH), − 21.93 and –22.33 ($\boldsymbol{Si}CH_3$). ^{13}C NMR (CH_3OD): δ (ppm) = 141.08 ($\boldsymbol{C}H_2$=CH), 133.78 (CH_2=$\boldsymbol{C}$H) 68.80 ($SiCH_2CH_2\boldsymbol{C}H$), 66.35 ($\boldsymbol{CH_2}N\boldsymbol{CH_2}$), 49.79 (N$\boldsymbol{C}$H), 23.49 ($Si\boldsymbol{C}H_2CH_2$), 19.88 ($NCH_2\boldsymbol{C}H_2$), 15.85 ($SiCH_2\boldsymbol{C}H_2$), 1.42 ($Si(\boldsymbol{C}H_3)_3$), 0.76 ($Si\boldsymbol{C}H_3$). IR (KBr, cm^{-1}): 3065, 2955, 2897, 1665, 1471, 1258, 1085, 879, 754. ESI–MS: calculated, 372.22 $g{\cdot}mol^{-1}$; found, 372.23.

2.8 Apparatus and Procedures

^{1}H NMR spectra were recorded using a Bruker AV 300 spectrometer in chloroform-d ($CDCl_3$) or methanol-d (CD_3OD). FT-IR were recorded using a VERTEX 70 FT-IR spectrometer. Measurements were performed on samples dispersed in anhydrous KBr pellets.

Surface tension measurements were carried out on a model BZY-1 tensiometer (Shanghai Hengping Instrument Co., Ltd., accuracy ± 0.1 $mN{\cdot}m^{-1}$) using a thermostatic bath. All measurements were repeated until the values were reproducible. Temperature was controlled at 25 ± 0.1 °C by a thermostatic bath. Calibration was performed using a liquid with known values of surface tension.

Specific conductivity measurements on the aqueous solutions were performed by using a low-frequency conductivity analyzer (model DDS-307, Shanghai Precision & Scientific Instrument Co., Ltd., accuracy ± 1%). Temperature was controlled at 15 ± 0.1, 20 ± 0.1, 25 ± 0.1, 30 ± 0.1, and 35 ± 0.1 °C by a thermostatic bath. The conductivity cell was calibrated with KCl solutions, and the cell constants were determined at the investigated temperatures.

Transmission electron microscopy (TEM) experiments were performed with a JEOL JEM-100 CXII (Japan) operating at 100 kV. The samples were prepared by placing the solutions on a copper TEM grid. A drop of phosphotungstic acid solution (2 wt%) was used to stain the samples when the grids were dried at room temperature.

3 Results and Discussion

3.1 Surface Tension Measurements

The surface tensions (γ) of the three synthesized trisiloxane surfactants, Et-Si_3PyCl, Vi-Si_3PyCl, and Si_3PyCl, in aqueous solution, were measured at 25 °C. Figure 2 shows the plots of surface tensions for the three cationic trisiloxane surfactants as functions of the molar concentration (C). As shown in Fig, 2, the surface tension decreases initially with increasing concentration of cationic silicone surfactant, indicating that the surfactants are adsorbed at the air/water interface. Then a plateau appears in the γ versus C plot, suggesting that micelles are formed. The concentration of the break point was considered as the critical micelle concentration (*CMC*), and the CMC values are given in Table 1.

In Table 1, the *CMC* values of cationic trisiloxane surfactants follow the order Et-Si_3PyCl < Vi-Si_3PyCl < Si_3PyCl. This is because Si_3PyCl can efficiently assemble at the air/solution interface to form dense surface films packed with smaller trimethylsiloxyl groups. Et-Si_3PyCl has larger triethylsiloxyl groups with more distinct steric hindrance compared with Vi-Si_3PyCl (dimethylvinylsiloxyl) [20].

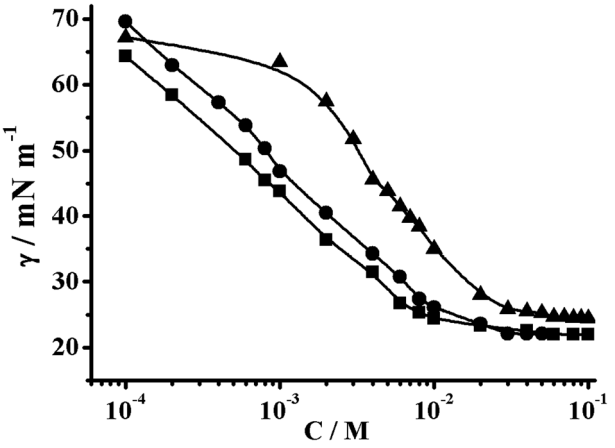

Fig. 2 Surface tension of Et-Si_3PyCl (filled square), Vi-Si_3PyCl (filled circle), and Si_3PyCl (filled triangle) in aqueous solutions as a function of their concentrations at 25 °C

Table 1 Critial micelle concentration (*CMC*) and adsorption parameters of Et-Si_3PyCl, Vi-Si_3PyCl, and Si_3PyCl in aqueous solutions at 25 °C

	CMC[a]	*CMC*[b]	γ_{cmc} (mN·m^{-1})	Π_{cmc} (mN·m^{-1})	pC_{20}	Γ_{max} (μmol·m^{-2})	A_{min} (Å^2)
Si_3PyCl	23.9	24.5	24.5	48.0	2.54	2.48	67.0
Vi-Si_3PyCl	13.5	14.2	22.3	50.2	3.16	2.05	81.3
Et-Si_3PyCl	10.4	10.9	22.1	50.4	3.37	1.83	90.8

[a]Determined from surface tension

[b]Determined from electrical conductivity

Generally, three parameters, the surface tension at *CMC* (γ_{CMC}), the adsorption efficiency (pC_{20}) and surface pressure at *CMC* (Π_{CMC}), which can be obtained from the surface tension plot, are utilized to evaluate the surface activities of the three cationic trisiloxane surfactants. The adsorption efficiency (pC_{20}) can be obtained by Eq. 1 and the results are listed in Table 1

$$pC_{20} = -\log C_{20} \tag{1}$$

where C_{20} denotes the concentration required to reduce the surface tension of pure solvent by 20 mN·m^{-1}. The larger the pC_{20} value, the higher is the adsorption efficiency of the surfactant [15, 21]. It can be seen that the values of pC_{20} increase in the order Et-Si_3PyCl > Vi-Si_3PyCl > Si_3PyCl.

The surface pressure at *CMC*, Π_{CMC}, is defined by Eq. 2 [15, 22]

$$\Pi_{CMC} = \gamma_0 - \gamma_{CMC} \tag{2}$$

where γ_0 is the surface tension of pure water and γ_{CMC} is the surface tension at the *CMC*. So, the values of Π_{CMC} indicate the maximum reduction of surface tension, and it becomes a measure of the effectiveness of the silicone surfactant to lower the surface tension of water [23]. As seen in Table 1, the γ_{CMC} values of Et-Si_3PyCl, Vi-Si_3PyCl and Si_3PyCl solutions are 22.1, 22.3, and 24.5 mN·m^{-1}, respectively, and are lower γ_{CMC} values than those of conventional ionic surfactants, i.e., hexadecyltrimethylammonium chloride (γ_{CMC} = 41.0) and octadecyltrimethylammonium bromide (γ_{CMC} = 35.0) [24]. Meanwhile, their Π_{CMC} values are larger than those of conventional cationic surfactants, suggesting that

the surface activities of the three cationic trisiloxane surfactants are greater than those of hydrocarbon surfactants, i.e., alkyl trimethylammonium bromides/chlorides and alkyl imidazolium bromides. This is attributed to the unique flexibility of the Si–O–Si backbone leading the silicone surfactants to adopt various configurations at the air/solution interface [15]. It was found that the values of pC_{20} and Π_{CMC} of Et-Si_3PyCl are the largest, which indicates that the efficiency and effectiveness of Et-Si_3PyCl are remarkable.

Based on the Gibbs adsorption isotherm, the maximum excess surface concentration (Γ_{max}) and the area occupied by a single cationic silicone surfactant molecule at the air/water interface (A_{min}) can be obtained and reflect the surface arrangement of surfactants at the air/liquid interface [25]. The maximum excess surface concentration, Γ_{max}, is calculated from Eq. 3 [26]:

$$\Gamma_{\max} = -\frac{1}{nRT}\left(\frac{\partial\gamma}{\partial \ln C}\right) \tag{3}$$

where γ is the surface tension, R is the ideal gas constant, T is the absolute temperature, $\frac{\partial\gamma}{\partial \ln C}$ is the slope of the linear fit of the data before the *CMC* in the surface tension plots, and n is the number of ionic species, respectively. For 1:1 ionic surfactants in the absence of any other solutes, n is equal to 2. Then, A_{min} is calculated by Eq. 4 [26]

$$A_{\min} = \frac{10^{16}}{N_A \Gamma_{\max}} \tag{4}$$

where N_A is Avogadro's number. Then, the values of Γ_{max} and A_{min} were gotten and are listed in Table 1. A higher value of Γ_{max} or lower value of A_{min} reveal a denser arrangement of surfactant molecules at the surface of the solution [25].

The A_{min} values are 90.8, 81.3, and 67.0 Å^2 for Et-Si_3PyCl, Vi-Si_3PyCl, and Si_3PyCl, respectively, and the values are lower than those of cationic silicone surfacetants, i.e., 3-[tri-(trimethylsiloxy)]silylpropylpyridiniumchloride (A_{min} = 117.8 Å^2) and *N*-methyl-3-[tri-(trimethylsiloxy)]silylpropylpiperidinium chloride (A_{min} = 100.7 Å^2). The reason may be that less branched silyoxyl groups promoted a denser arrangement among the silicone surfactant molecules. Meanwhile, the larger A_{min} value of Et-Si_3PyCl compared with Vi-Si_3PyCl and Si_3PyCl can be attributed to the steric hindrance of the triethylsilyoxyl groups. This reveals a dense arrangement for the cationic silicone surfactant molecules at the air/water interface [27].

4 Thermodynamic Analysis of Micellization

The thermodynamic analyses of Et-Si_3PyCl, Vi-Si_3PyCl, and Si_3PyCl in aqueous solution were carried out with use of electric conductivity measurements. The electrical conductivity, κ, as a function of surfactant concentration for Et-Si_3PyCl, Vi-Si_3PyCl, and Si_3PyCl at several different temperatures, are shown in Fig. 3. The *CMC* values were estimated from the intersection of the two straight lines in $\kappa - C$ plots and are listed in Table 2. Obviously, the *CMC* values at 25 °C are in good accordance with those obtained from surface tension measurement (see Table 1). As shown in Table 2, the *CMC* values increase with increasing temperature, and this phenomenon is affected by two factors. Higher temperature may decrease the degree of hydration of the pyrrolidinium groups, which is beneficial to micelle formation. As the temperature increases, however, the water structure surrounding the

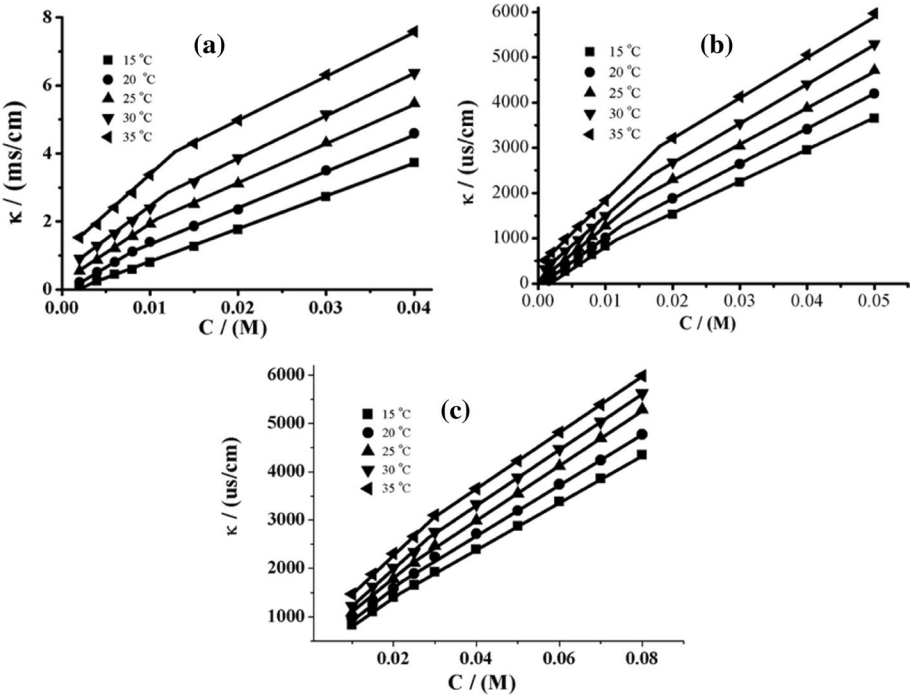

Fig. 3 Specific conductivity as a function of concentration at different temperatures: **a** Et-Si_3PyCl, **b** Vi-Si_3PyCl, and **c** Si_3PyCl

Table 2 Critial micelle concentration (*CMC*), degree of counterion binding (β) and thermodynamic parameters of Et-Si_3PyCl, Vi-Si_3PyCl, and Si_3PyCl in aqueous solutions at different temperatures

Surfactants	T (°C)	*CMC* (mmol·L^{-1})	β	ΔG_m^o (kJ·mol^{-1})	ΔH_m^o (kJ·mol^{-1})	$-T\Delta S_m^o$ (kJ·mol^{-1})
Et-Si_3PyCl	15	3.5 ± 0.1	0.45 ± 0.01	− 28.63 ± 0.11	9.35 ± 0.011	− 37.99 ± 0.10
	20	8.0 ± 0.1	0.36 ± 0.01	− 28.07 ± 0.10	6.75 ± 0.008	− 34.81 ± 0.10
	25	10.9 ± 0.1	0.32 ± 0.01	− 27.93 ± 0.09	4.22 ± 0.005	− 32.16 ± 0.09
	30	12.0 ± 0.1	0.30 ± 0.01	− 28.83 ± 0.09	1.79 ± 0.002	− 30.62 ± 0.09
	35	12.9 ± 0.1	0.23 ± 0.01	− 31.07 ± 0.10	− 0.57 ± 0.001	− 30.50 ± 0.11
Vi-Si_3PyCl	15	11.7 ± 0.1	0.39 ± 0.01	− 25.63 ± 0.08	23.24 ± 0.028	− 48.88 ± 0.05
	20	12.6 ± 0.1	0.37 ± 0.01	− 26.39 ± 0.09	20.40 ± 0.024	− 46.79 ± 0.06
	25	14.2 ± 0.1	0.34 ± 0.01	− 27.29 ± 0.10	17.65 ± 0.021	− 44.94 ± 0.08
	30	17.0 ± 0.1	0.29 ± 0.01	− 27.91 ± 0.12	14.99 ± 0.018	− 42.90 ± 0.09
	35	18.1 ± 0.1	0.26 ± 0.01	− 28.65 ± 0.14	12.42 ± 0.015	− 41.06 ± 0.12
Si_3PyCl	15	21.7 ± 0.1	0.28 ± 0.01	− 22.10 ± 0.11	28.07 ± 0.033	− 50.16 ± 0.07
	20	22.1 ± 0.1	0.25 ± 0.01	− 23.39 ± 0.12	18.60 ± 0.022	− 41.99 ± 0.09
	25	24.5 ± 0.1	0.24 ± 0.01	− 23.68 ± 0.13	9.45 ± 0.011	− 33.13 ± 0.12
	30	28.4 ± 0.1	0.23 ± 0.01	− 23.79 ± 0.16	0.60 ± 0.001	− 24.39 ± 0.16
	35	29.6 ± 0.1	0.18 ± 0.01	− 24.70 ± 0.14	− 7.96 ± 0.009	− 16.74 ± 0.13

silicone groups may be destroyed, which may slow micelle formation [28, 29]. It is clear that the latter effect plays a crucial role in the micellization process for these systems.

The degree of counterion binding of micelles can also be estimated form conductivity measurements by Eq. 5 [26]:

$$\beta = 1 - \frac{\alpha_1}{\alpha_2} \tag{5}$$

where α_1 and α_2 are the slopes of the straight lines before and after the *CMC* in $\kappa - C$ plots, respectively. The β values for Et-Si_3PyCl, Vi-Si_3PyCl, and Si_3PyCl obtained from conductivity measurements at different temperatures are summarized in Table 2. It can be seen that the β values of Et-Si_3PyCl, Vi-Si_3PyCl, and Si_3PyCl are all pretty low, signifying that the self-repulsion is stronger than the attraction between the head groups and counterions. Additionally, it is noteworthy that the small break in the $\kappa - C$ plots for Si_3PyCl is similar with the observation by Tsubone et al. [30].

The thermodynamic parameters of micellization for Et-Si_3PyCl, Vi-Si_3PyCl, and Si_3PyCl, such as the standard Gibbs energy change (ΔG^o_m), the standard entropy change (ΔS^o_m), and the standard enthalpy change (ΔH^o_m), were estimated based on the mass action model [31], in order to understand the effect of the hydrophobic chain on the micellization of the three cationic trisiloxane surfactants. Values of ΔG^o_m can be obtained from Eq. 6 [15, 26, 30]

$$\Delta G^o_m = (1 + \beta) RT \ln \chi_{cmc} \tag{6}$$

where χ_{CMC} is the mole fraction of silicone surfactant at the *CMC*, T is the absolute temperature, and R is the ideal gas constant. Thus, the enthalpy and entropy of micelle formation can be calculated by the Gibbs–Helmholtz equation (Eqs. 7 and 8)

$$\Delta H^o_m = \left[\frac{\partial (\Delta G^o_m / T)}{\partial (1/T)} \right] \tag{7}$$

$$\Delta S^o_m = \frac{\Delta H^o_m - \Delta G^o_m}{T} \tag{8}$$

The thermodynamic parameters for Et-Si_3PyCl, Vi-Si_3PyCl, and Si_3PyCl are given in Table 2.

In the whole investigated temperature range, all the ΔG^o_m values for Et-Si_3PyCl, Vi-Si_3PyCl, and Si_3PyCl are negative. Meanwhile, the ΔG^o_m values follow the order Et-Si_3PyCl > Vi-Si_3PyCl > Si_3PyCl, owning to decreasing in the hydrophobic effect of siloxane hydrophobic groups for Et-Si_3PyCl, Vi-Si_3PyCl, and Si_3PyCl, respectively.

As can be seen in Table 2 and Fig. 4, the ΔH^o_m values for Vi-Si_3PyCl are positive within the investigated temperature range. However, the values of ΔH^o_m for Et-Si_3PyCl and Si_3PyCl are positive at low temperatures and become negative at higher temperatures. The change observed is similar to that of many ionic surfactants. During the micellization process, positive values mean the release of structured water from the hydration layer around the hydrophobic parts of the molecule. The values of ΔH^o_m are negative, indicating the London dispersion interactions are considered to be attractive forces. In contrast, values of ΔH^o_m are positive, suggesting the iceberg-structured water around the siloxane hydrophobic groups of trisiloxane surfactants was destroyed. This prompted the silicone surfactants–solution system to have more disorder, resulting in a positive contribution to the values of ΔS^o_m [32–35]

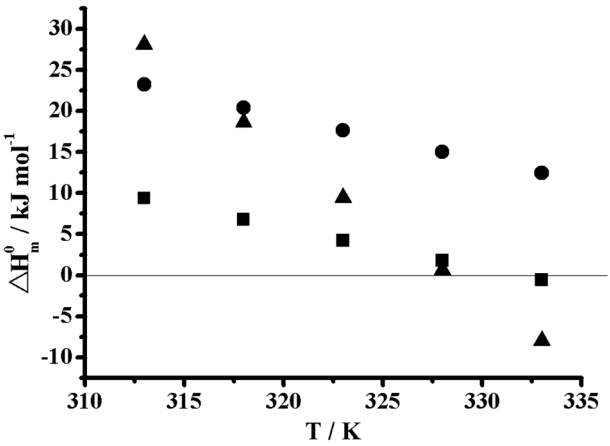

Fig. 4 Enthalpy of micellization for Et-Si_3PyCl (filled square), Vi-Si_3PyCl (filled circle), and Si_3PyCl (filled triangle) as a function of temperature

The values of ΔS_m^o for Et-Si_3PyCl, Vi-Si_3PyCl, and Si_3PyCl are positive in the whole investigated temperature range and decrease with temperature increase. The positive ΔS_m^o values are caused by the increased disorder of the siloxane hydrophobic chains in the micellar core and the destruction of iceberg-structured water around the hydrophobic parts of trisiloxnae surfactants. During the aggregation process of the cationic silicone surfactants in aqueous solution, the siloxane–water interactions in aqueous solutions of trisiloxane surfactant monomers are replaced by siloxane–siloxane interactions inside the trisiloxane surfactant micelles. In other words, the highly ordered structure of water around the siloxane chain of the trisiloxane surfactant in the monomeric form was replaced by a looser structure in the interior of the aggregation [32–35].

Furthermore, it is worth noting that the values of ΔG_m^o for Et-Si_3PyCl, Vi-Si_3PyCl, and Si_3PyCl are all mainly contributed by $-\Delta TS_m^o$ over the whole temperature range. That indicates the micellization process for Et-Si_3PyCl, Vi-Si_3PyCl, and Si_3PyCl in aqueous solution is entropy driven, which may be the result of the siloxane hydrophobic group transfer from the water phase to the inside of the micelle. In addition, Et-Si_3PyCl, Vi-Si_3PyCl, and Si_3PyCl in aqueous solution can form non-uniform sizes of spheroidal aggregates as observed by TEM (seen in Fig. 5).

As mentioned above, the structures of the siloxane hydrophobic groups of the cationic trisiloxane surfactants have significant influence on the driving force for aggregate formation.

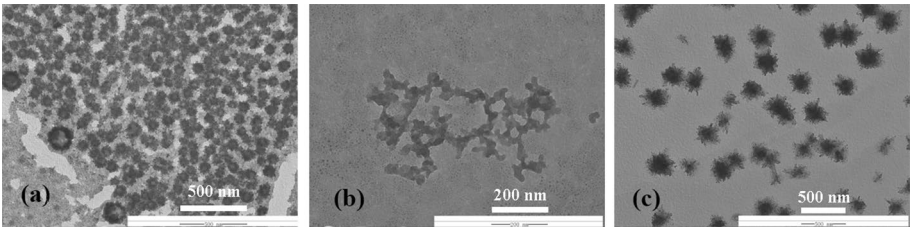

Fig. 5 TEM images of aggregates of Et-Si_3PyCl (**a**), Vi-Si_3PyCl (**b**), and Si_3PyCl (**c**)

5 Conclusions

The surface activities and thermodynamic analysis of three trisiloxane surfactants with different siloxane hydrophobic groups (trimethylsiloxyl, dimethylvinylsiloxyl, and triethylsiloxyl) were investigated in aqueous solution. The three cationic trisiloxane surfactants have excellent surface activity compared with common hydrocarbon surfactants due to the superior properties of silicone. The structures of siloxane hydrophobic groups can obviously influence their surface activities and thermodynamics. The *CMC* values increase following the order Et-Si_3PyCl < Vi-Si_3PyCl < Si_3PyCl. Also, Et-Si_3PyCl packs more loosely at the air/water interface owing to the steric hindrance of triethylsilyoxyl groups. The ΔG_m^o values increase in the order Et-Si_3PyCl > Vi-Si_3PyCl > Si_3PyCl, which is attributed to the decrease in the hydrophobic effect. The micellization process for Et-Si_3PyCl, Vi-Si_3PyCl, and Si_3PyCl are entropy-driven, caused by the tendency of the siloxane hydrophobic group to transfer from the water phase to the inside of the micelle.

Acknowledgements We gratefully acknowledge the financial support from the National Natural Science Foundation of China (No. 21563016).

References

1. Hill, R.M.: Silicone Surfactants. Marcel Dekker, New York (1999)
2. Hill, R.M.: Silicone surfactants—New development. Curr. Opin. Colloid Interface Sci. **7**, 255–261 (2002)
3. Peter, J.G.: Organosilicon surfactants as adjuvants for agrochemicals. Pestic. Sci. **38**, 103–122 (1993)
4. Churaev, N.V., Esipova, N.E., Hill, R.M., Sobolev, V.D., Starov, V.M., Zorin, Z.M.: The superspreading effect of trisiloxane surfactant solutions. Langmuir **17**, 1338–1348 (2001)
5. Hill, R.M., Svitova, T., Smirnova, Y., Stuermer, A.: Wetting and interfacial transitions in dilute solutions of trisiloxane surfactants. Langmuir **14**, 5023–5031 (1998)
6. Harald, W., Knudsen, K.D.: Microstructures in aqueous solutions of a polyoxyethylene trisiloxane surfactant and a cosurfactant studied by SANS and NMR self-diffusion. Langmuir **24**, 10637–10645 (2008)
7. Bonnington, L., Henderson, S.W., Zabkiewicz, J.A.: Characterization of synthetic and commercial trisiloxane surfactant materials. Appl. Organomet. Chem. **18**, 28–38 (2004)
8. Du, Z.P., Li, E., Cao, Y., Li, X., Wang, G.: Synthesis of trisiloxane-tailed surface active ionic liquids and their aggregation behavior in aqueous solution. Colloids Surf. A **441**, 744–751 (2014)
9. Li, P., Du, Z.P., Ma, X.Y., Wang, G.Y., Li, G.J.: Synthesis, adsorption and aggregation properties of trisiloxane room-temperature ionic liquids. J. Mol. Liq. **192**, 38–43 (2014)
10. Qin, J.Q., Du, Z.P., Ma, X.Y., Zhu, Y.Y., Wang, G.Y.: Effect of siloxane backbone length on butynediol-ethoxylate based polysiloxanes. J. Mol. Liq. **214**, 54–58 (2016)
11. Wang, G.Y., Li, X., Du, Z.P., Li, E.Z., Li, P.: Butynediol-ethoxylate based trisiloxane: structural characterization and physico-chemical properties in water. J. Mol. Liq. **197**, 197–203 (2014)
12. Sakai, K., Tamura, M., Umezawa, S., Takamatsu, Y., Torigoe, K., Yoshimura, T., Esumi, K., Sakai, H.: Adsorption characteristics of sugar-based monomeric and gemini surfactants at the silica/aqueous solution interface. Colloids Surf. A **328**, 100–106 (2008)
13. EL-Sukkary, M., Ismail, D., Rayes, S.E., Saad, M.: Synthesis, characterization and surface properties of amino-glycopolysiloxane. J. Ind. Eng. Chem. **20**, 3342–3348 (2014)
14. Zhao, X.H., Liang, W.P., An, D., Ye, Z.W.: Synthesis and properties of tetrasiloxane Gemini imidazolium surfactants. Colloid Polym. Sci. **294**, 491–500 (2016)
15. Tan, J.L., Ma, D.P., Feng, S.Y., Zhang, C.Q.: Effect of headgroups on the aggregation behavior of cationic silicone surfactants in aqueous solution. Colloids Surf. A **417**, 146–153 (2013)
16. Tan, J.L., Zhao, P.J., Ma, D.P., Feng, S.Y., Zhang, C.Q.: Effect of hydrophobic chains on the aggregation behavior of cationic silicone surfactants in aqueous solution. Colloid Polym. Sci. **291**, 1487–1494 (2013)

17. Tan, J.L., Feng, S.Y.: Effect of counterions on micellization of pyrrolidinium based silicone ionic liquids in aqueous solutions. J. Chem. Eng. Data **59**, 1830–1834 (2014)
18. Fang, L.Y., Tan, J.L., Zheng, Y., Li, H.N., Li, C.W., Feng, S.Y.: Effect of organic salts on the aggregation behavior of tri-(trimethylsiloxy)silylpropylpyridinium chloride in aqueous solution. Colloids Surf. A **509**, 48–55 (2016)
19. Fang, L.Y., Tan, J.L., Zheng, Y., Yang, G., Yu, J.T., Feng, S.Y.: Synthesis, aggregation behavior of novel cationic silicone surfactants in aqueous solution and their application in metal extraction. J. Mol. Liq. **231**, 134–141 (2017)
20. Czajka, A., Hazell, G., Eastoe, J.: Surfactants at the design limit. Langmuir **31**, 8205–8217 (2015)
21. Zhang, S.H., Yan, H., Zhao, M.W., Zheng, L.Q.: Aggregation behavior of gemini pyrrolidine-based ionic liquids 1,1′-(butane-1,4-diyl)bis(1-alkylpyrrolidinium) bromide ([Cnpy-4-Cnpy][Br 2]) in aqueous solution. J. Colloid Interf. Sci. **372**, 52–57 (2012)
22. Brown, P., Butts, C., Dyer, R., Eastoe, J., Grill, I., Guittard, F., Rogers, S.: Anionic surfactants and surfactant ionic liquids with quaternary ammonium counterions. Langmuir **27**, 4563–4571 (2011)
23. Dong, B., Zhao, X.Y., Zheng, L.Q., Inoue, T.: Aggregation behavior of long-chain imidazolium ionic liquids in aqueous solution: micellization and characterization of micelle microenvironment. Colloids Surf. A **317**, 666–672 (2008)
24. Mata, J., Varade, D., Bahadur, P.: Aggregation behavior of quaternary salt based cationic surfactants. Thermochim. Acta **428**, 147–155 (2005)
25. Jaycock, M.J., Parfitt, G.D.: Chemistry of Interfaces. Wiley, New York (1981)
26. Rosen, M.J.: Surfactants and Interfacial Phenomena. Wiley, New York (1989)
27. Rao, K.S., Singh, T., Trivedi, T.J., Kumar, A.: Aggregation behavior of amino acid ionic liquid surfactants in aqueous media. J. Phys. Chem. B **115**, 13847–13853 (2011)
28. Shi, L.J., Li, N., Yan, H., Gao, Y.A., Zheng, L.Q.: Aggregation behavior of long-chain *N*-aryl imidazolium bromide in aqueous solution. Langmuir **27**, 1618–1625 (2011)
29. Zhang, Q., Gao, Z.N., Xu, F.S., Tai, X.J.: Effect of hydrocarbon structure of the headgroup on the thermodynamic properties of micellization of cationic gemini surfactants: an electrical conductivity study. J. Colloid Interface Sci. **371**, 73–81 (2012)
30. Tsubone, K., Arakawa, Y., Rosen, M.J.: Structural effects on surface and micellar properties of alkanediyl-α, ω-bis(sodium *N*-acyl-β-alaninate) gemini surfactants. J. Colloid Interface Sci. **262**, 516–524 (2003)
31. Olutas, E.B., Aamis, M.J.: Thermodynamic parameters of some partially fluorinated and hydrogenated amphiphilic enantiomers and their racemates in aqueous solution. Chem. Thermodyn. **47**, 144–153 (2012)
32. Zieliński, R.: Effect of temperature on micelle formation in aqueous NaBr solutions of octyltrimethylammonium bromide. J. Colloid Interface Sci. **235**, 201–209 (2001)
33. Wu, S.Y., Yan, Z.N., Wen, X.L., Xu, C.Y., Pan, Q.: Conductometric and fluorescence probe investigations of molecular interactions between dodecyltrimethylammonium bromide and dipeptides. Colloid Polym. Sci. **292**, 2775–2783 (2014)
34. Kiràly, Z., Dekàny, I.: A thermometric yitration study on the micelle formation of sodium decyl sulfate in water. J. Colloid Interface Sci. **242**, 214–219 (2001)
35. Šarac, B., Bešter-Rogac, M.: Temperature and salt-induced micellization of dodecyltrimethylammonium chloride in aqueous solution: a thermodynamic study. J. Colloid Interf. Sci. **338**, 216–221 (2009)